

SIMULATION STUDIES AND EXPERIMENTAL RESEARCH OF OMNIDIRECTIONAL TRACKED VEHICLE¹

MATEUSZ FIEDEN, JACEK BALCHANOWSKI

Wrocław University of Science and Technology, Wrocław, Poland

e-mail: mateusz.fieden@pwr.edu.pl; jacek.balchanowski@pwr.edu.pl

The article focuses on the control of an omni-tracked vehicle in a symmetrical fully overlapping track system. The vehicle in question is equipped with four independently controlled tracks. The links of each crawler are equipped with a single rolling roller, fixed at an angle to the direction of the vehicle main axis. The authors propose mathematical description to determine the direction and speed of movement of a single pair of omni-tracks with oppositely arranged rolling rollers. Numerical tests were carried out, the results of which were compared with the mathematical model. The numerical studies were then subjected to experimental verification, using a full-scale prototype. A dynamic direction correction algorithm was also proposed with its effectiveness proved experimentally.

Keywords: kinematic, omnidirectional, omnitank, omnitracks, omnivehicle

1. Introduction

Omnidirectional vehicles and drives that enable this type of motion have been present in mechanics for more than 100 years (Grabowiecki, 1919). Wheeled robots equipped with Swedish wheels, or mecanum wheels, have been known for many years, so knowledge about them is extensive and mathematical descriptions are accurate (Bae and Kang, 2016; Taheri and Zhao, 2020; Yamada *et al.*, 2017). However, there is a certain group of omnidirectional vehicles that has appeared in scientific studies only recently – omnidirectional tracked vehicles. These vehicles are equipped with a variation of typical link-composed tracks, in which each link is equipped with at least one free rolling roller located at an appropriate angle with respect to the main axis of the track. An example of such a roller is shown in Fig. 1. Vehicles equipped with such tracks

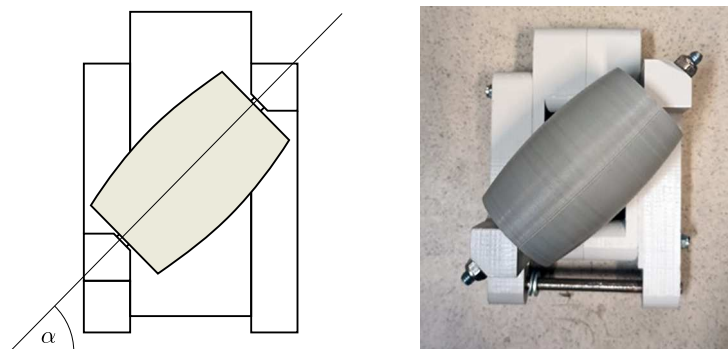


Fig. 1. Omnidirectional track link with a single rolling roller mounted at an angle α

can be divided according to the mutual orientation of the rollers and the mutual orientation of the entire track segments (Zhang *et al.*, 2018). There are also separate groups of omnidirectional

¹Paper presented during PCM-CMM 2023, Gliwice, Poland

vehicles equipped with transverse active drive rollers (Takaduma *et al.*, 2008, 2018; Takaneetal, 2019).

Vehicles with non-parallel tracks have been present in the literature for more than 20 years. The article (Isoda *et al.*, 1999) presents the concept of a vehicle with four tracks. The tracks are arranged in a square plan. Each track has an independent drive. The rollers are located at $\alpha = 90^\circ$ to the longitudinal axis of the track. Further testing of the vehicle is presented in the paper (Chen *et al.*, 2002), where dynamic analysis of the model, the proposed control system and the results of off-road runs of the prototype were presented. A similar concept was presented by Bruton (2023). Vehicle proposed by author is equipped with tracks with rollers fixed at $\alpha = 90^\circ$. The track segments are arranged in the plan of an equilateral triangle. Vehicles with non-parallel tracks have one common feature: during translational movement, regardless of its direction, free rolling rollers are used to roll the vehicle body. For this reason, the potential of vehicles in question to overcome off-road obstacles, as well as to navigate difficult terrain, can be significantly reduced, although these vehicles are theoretically still tracked vehicles. A separate group is tracked vehicles with parallel tracks. Unlike the previously described group, there is no rotational movement of the free rolling rollers during movement in the main axis, which allows the features of a classic tracked vehicle to be maintained. The division of omnidirectional vehicles with parallel tracks is presented in Fig. 2.

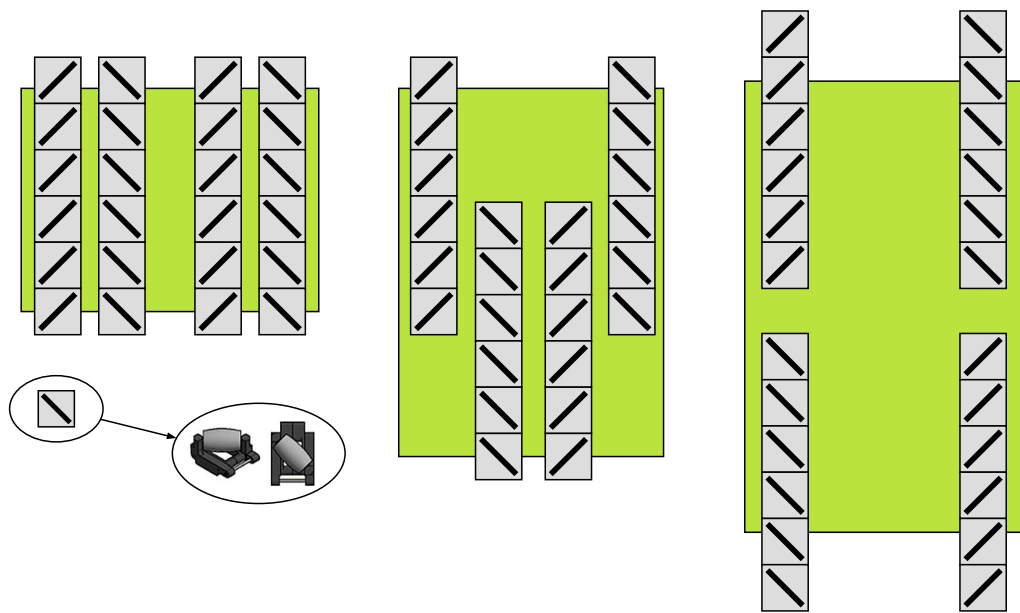


Fig. 2. Diagram of the arrangement of free rolling rollers in different types of omni-track vehicles. From left: fully overlapping, partially overlapping and non-overlapping tracks. In all examples, the distribution of rollers is longitudinally symmetrical

In the literature, the most widely described group of vehicles with parallel tracks are vehicles with fully non-overlapping tracks. The article (Zhang and Huang, 2015) presents theoretical considerations on the kinematics of vehicles with tracks with free rolling rollers in both parallel and non-parallel systems. It presents field tests of a prototype of the vehicle in question, including the current consumption of various drives during different types of movement and the relationship between the angular orientation of the robot and its ability to overcome terrain obstacles. In (Mortensen Ernits *et al.*, 2017), the authors present tests conducted on two built omni-track vehicles. The first of these had dimensions of $0.8\text{ m} \times 1.2\text{ m}$, while the second was $2.5\text{ m} \times 3.5\text{ m}$. The article describes a series of experimental tests that were carried out on the proposed demonstrators. The tests consisted of traversing preset trajectories that took into

account a change in the angular orientation of the body and movement in different directions. Theoretical considerations on the potential application of such vehicles are presented.

The work presented in (Fang *et al.*, 2020) includes numerical testing of a full-scale prototype of an omni-tracked vehicle. The equations of kinematics for this type of chassis, as well as analysis of the effect of the angular orientation of the rolling roll on the obtained motion speeds were presented. In the numerical tests, linear motion in different directions and motion folding of the prototype vehicle were simulated and described. In addition, the article provided experimental studies measuring the effect of movement direction and drives speed on the values of the current drawn by the drives. Tracked vehicles in a partially occurring system are described in (Zhang *et al.*, 2018), where simulation studies of such a vehicle are presented. The paper highlights the aspect of curvature of the motion trajectory when driving in a direction other than the main axis of the vehicle. This effect was confirmed in (Fang *et al.*, 2020; Fiedeń and Bałchanowski, 2021).

Vehicles with chassis in a fully overlapping track system are described in (Fiedeń and Bałchanowski, 2021). The authors presented the construction and testing of a lightweight prototype of the omni-tracked vehicle. The research included analysis of the trajectory of movement in the main axis and transverse axis, recorded on a bench equipped with a vision system. The paper proposes a method for counteracting the curvature of the trajectory of motion – the concept of static correction, which counteracts the unwanted rotation of the vehicle body by appropriately modifying the speed of individual drives. The results of tests confirm an improvement of the driving performance after applying the proposed correction algorithm.

The literature review revealed a significant research gap in the state of knowledge regarding omni-track vehicles. Many aspects of motion of such vehicles, for example, the compatibility of real models with theoretical models, the influence of design parameters on driving properties or adverse phenomena occurring during movement have been neglected or discussed and studied very narrowly (Fiedeń and Bałchanowski, 2022). The purpose of this paper is to discuss the unfavorable phenomenon of curvature of the trajectory of motion of an omni-track vehicle, as well as to present a proposed method to counteract this phenomenon.

2. Materials and methods

2.1. Design of kinematic model of an omnidirectional tracked vehicle and simulation research

Equations of kinematics have been proposed to determine the direction and speed of linear motion of a single omnidirectional track work. The starting point is the angular speed of drive wheels ω_r^1 and ω_r^2 with radius R . The individual vectors and the relationship between them are illustrated in Fig. 3.

The linear velocity of the track n ($n = 1-4$) denoted by v_{tr}^n , is calculated from the formula

$$v_{tr}^n = \omega_r^n R \quad (2.1)$$

The linear speed of the tracks can be decomposed into two components v_x^n and v_y^n . The component v_y^n is the same as the linear speed of the tracks, its direction is parallel to the track, and its value is

$$v_y^n = v_{tr}^n \quad (2.2)$$

The component v_x^n depends on the angular orientation of the free rolling roll, denoted by β , its direction is perpendicular to the track. For angles $\beta^1, \beta^3 = 135^\circ$ and $\beta^2, \beta^4 = 45^\circ$ it can be calculated from

$$v_x^n = \cot(\beta^n) v_{tr}^n \quad (2.3)$$

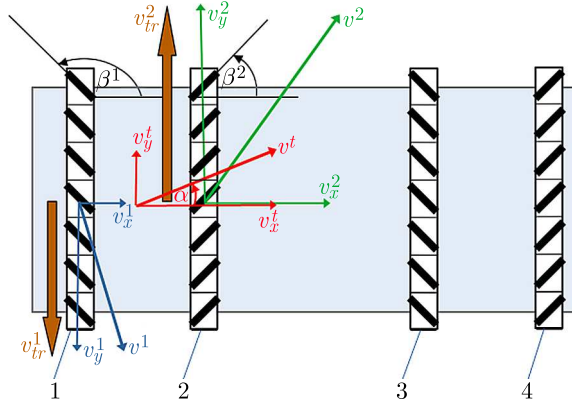


Fig. 3. Distribution of velocity vectors with designations

The velocity vector of a pair of tracks is denoted by v^t , and its angular orientation is denoted by α . The value of the velocity vector of the pair of tracks is

$$v^t = \sqrt{(v_x^t)^2 + (v_y^t)^2} \quad (2.4)$$

The values of the components, labeled v_x^t and v_y^t , depend on the values of the vectors v_x^n and v_y^n

$$v_x^t = \frac{v_x^1 + v_x^2}{2} \quad v_y^t = \frac{v_y^1 + v_y^2}{2} \quad (2.5)$$

The angular orientation α is expressed by the formula

$$\alpha = \arctan 2(v_y^t, v_x^t) \quad (2.6)$$

A solid model of a vehicle equipped with four linear drives was proposed. Each drive moved a single beam with attached free rolling rollers. Two rolling rollers were attached to each beam. The rollers were fixed at an angle $\beta^1, \beta^3 = 135^\circ$ and $\beta^2, \beta^4 = 45^\circ$ to the main axis of the model, and the way they were fixed along with the whole model, is shown in Fig. 4. The distance between the rollers was 200 mm. The total weight of the model was 20 kg. The distance between adjacent beams was 0.1 m.

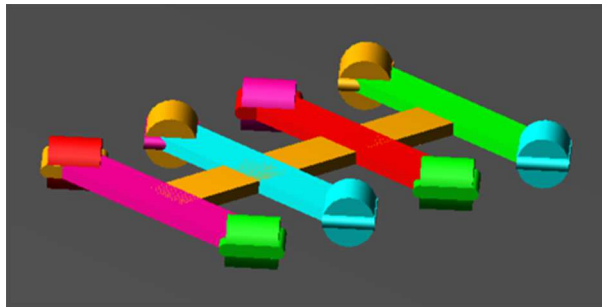


Fig. 4. A view of the simplified solid model of the omni-track vehicle

Dynamic contacts were formed between the rollers and the substrate. The contact parameters used for the simulation, selected based on (Engström *et al.*, 2010; Pasini, 2019), are shown in Table 1.

Based on the proposed equations, velocities were determined enabling the vehicle to move at selected angles. The displacements in time are given by a polynomial function with a smooth increment. The characteristics are shown in Fig. 5.

Table 1. Contact parameters between the substrate and the roller

Stiffness	20 N/mm	Static coefficient	1
Force exponent	2.2	Dynamic coefficient	1
Damping	0.001 Ns/mm	Stiction transition velocity	10 mm/s
Penetration depth	1 mm	Friction transition velocity	2000 mm/s

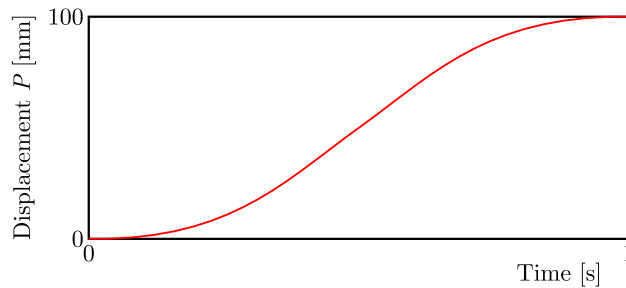


Fig. 5. Plot of the polynomial (Hexagon Adams STEP5 function) used as a control function in the drives of the proposed model

Table 2 shows the values of the speeds set for each drive, the expected orientation angles of the motion vector of the whole vehicle for these speeds, the expected speeds, and the orientation angle of the motion vector and speeds obtained by simulation. The t_s time of the simulation carried out was 1 s.

Table 2. Summary of set speeds of individual tracks, expected trajectory angles and obtained trajectory angles

ID	$v^1 = v^3$ [mm/s]	$v^2 = v^4$ [mm/s]	Expected trajectory angle [°]	Obtained trajectory angle [°]
a	-100	100	0.00	-0.19
b	-100	50	18.44	18.35
c	-100	0	45.00	45.01
d	-100	-50	71.56	71.56

Point P is located on the body of the robot. Figure 6 shows the obtained trajectory of the movement of point P during individual passes.

The simulations showed that the proposed model correctly reproduces the relationship between the rotational speeds of the drives and the direction of motion of the vehicle body. Therefore, it was reasonable to build a prototype with comparable design parameters for experimental verification of the obtained results.

2.2. Design of a prototype of an omnitracked vehicle and a research stand

To verify the correctness of numerical simulations, as well as the effectiveness of the proposed correction algorithm, a prototype omni-track vehicle was designed and manufactured. Then a measurement station equipped with a vision system was prepared.

The vehicle prototype consisted of four segments. Each segment was equipped with a crawler, one independent drive, drive wheel, tension wheel and road wheels. The kinematic diagram is shown in Fig. 7.

The projection of a single segment is shown in Fig. 8. Each segment consists of a single drive, which transmits torque to the drive wheel via a chain gear. A single track, consisting of 19 segments, is stretched between the drive and tension wheel. When moving on a flat surface at any time, a minimum of 6 rollers touch the ground. The weight of the vehicle is transferred

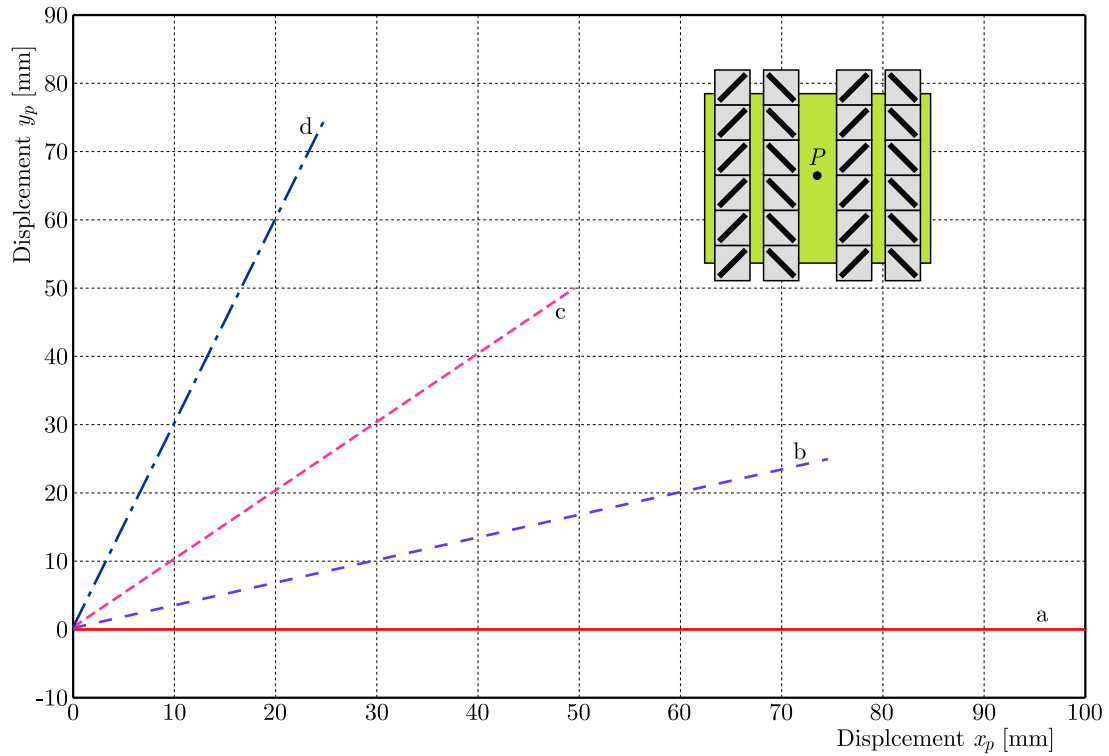


Fig. 6. Point P trajectories during individual runs $x_p y_p$

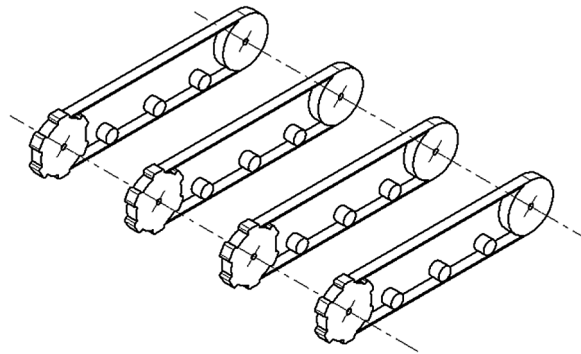


Fig. 7. Kinematic diagram of the prototype of an omni-track vehicle

to the ground via road wheels. This role is performed by road wheels and tension wheels, as well as three free wheels equipped with a spring-based compression system. A visualization of the prototype and a photo of the actual design are shown in Fig. 9. The basic design parameters of the robot are collected in Table 3.

Table 3. Basic design parameters of the robot

Roller diameter	50 mm	Drive wheel diameter	185 mm
Distance between drive and tension wheel	760 mm	Number of links in single track segment	19
Frame length	1050 mm	Frame width	960 mm
Weight	70 kg	Rated power of single drive	250 W

An AS5040 encoder with a resolution of 512 pulses per revolution was mounted on each drive, which, with the 9:16 gear used, allowed a theoretical resolution of less than 1 mm for measuring

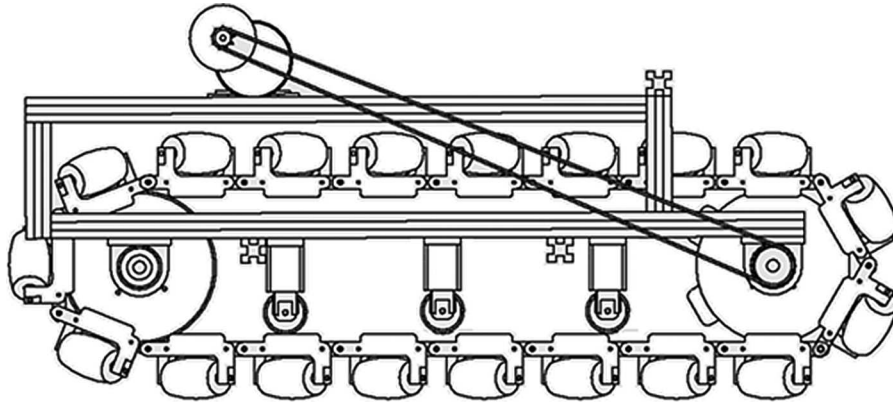


Fig. 8. Side view of a single track segment

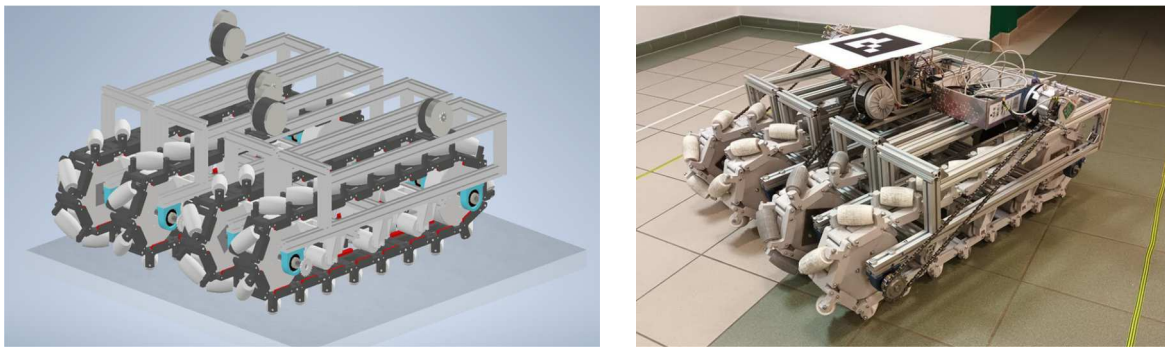


Fig. 9. Visualization of the prototype and a photo of the actual vehicle

linear motion of the track. An ATmega2560 microcontroller was used as the computational unit. Additional data on the vehicle angular orientation was provided by an NGIMU sensor. The control scheme of the vehicles is shown in Fig. 10. The robot can be controlled both by an operator, using RC apparatus, as well as by commands sent via UART.

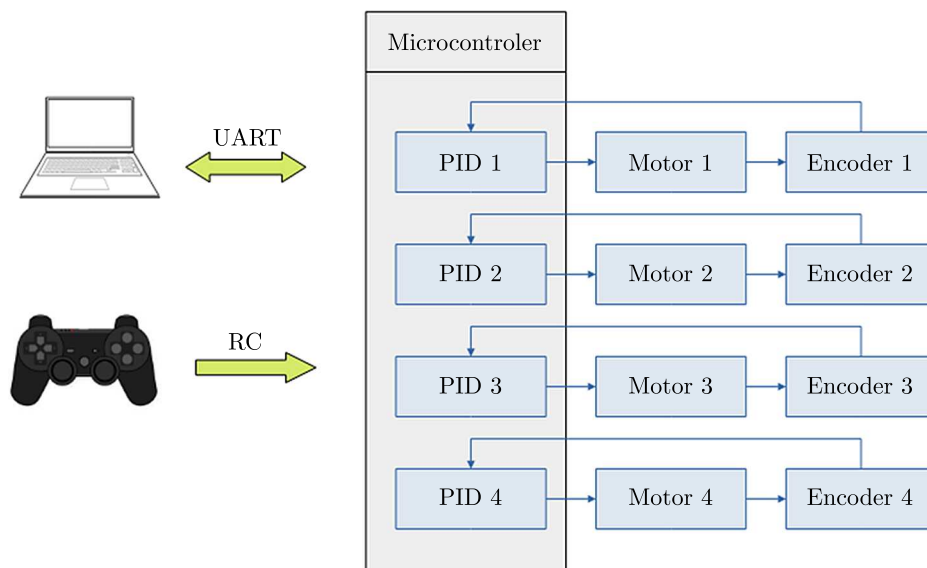


Fig. 10. General control scheme of the UART prototype

By equipping the prototype with an IMU sensor, it was possible to add an active direction compensation system. A schematic of the proposed system operation is shown in Fig. 11. The

variables i take values from 1 to 4, symbolizing successive drives. Variable φ_I is information about vehicle angular orientation at the time of takeoff, i.e. the yaw angle. This variable is transmitted once, before the start of movement. Variable φ_S is the stored initial angular orientation, which is to remain constant throughout the movement. Variable $\omega_i S$ are the set angular velocity values of individual drives. Variable $E\varphi$ is a difference between the actual and expected values of the vehicle angular orientation of the individual actuators. Analogically, $E\omega_i$ is a difference of angular velocity values. Variables $U\varphi$ and $U\omega_i$ are control signals, P_i describes values of the PWM signal that goes to the individual drives. Variables $\varphi(t)$ and $\omega(t)$ are the actual values of the actual angular orientation and angular velocity of the drives as measured by the IMU sensor and encoders. The $\omega_i S$ variable is the velocity reference value for the individual drives.

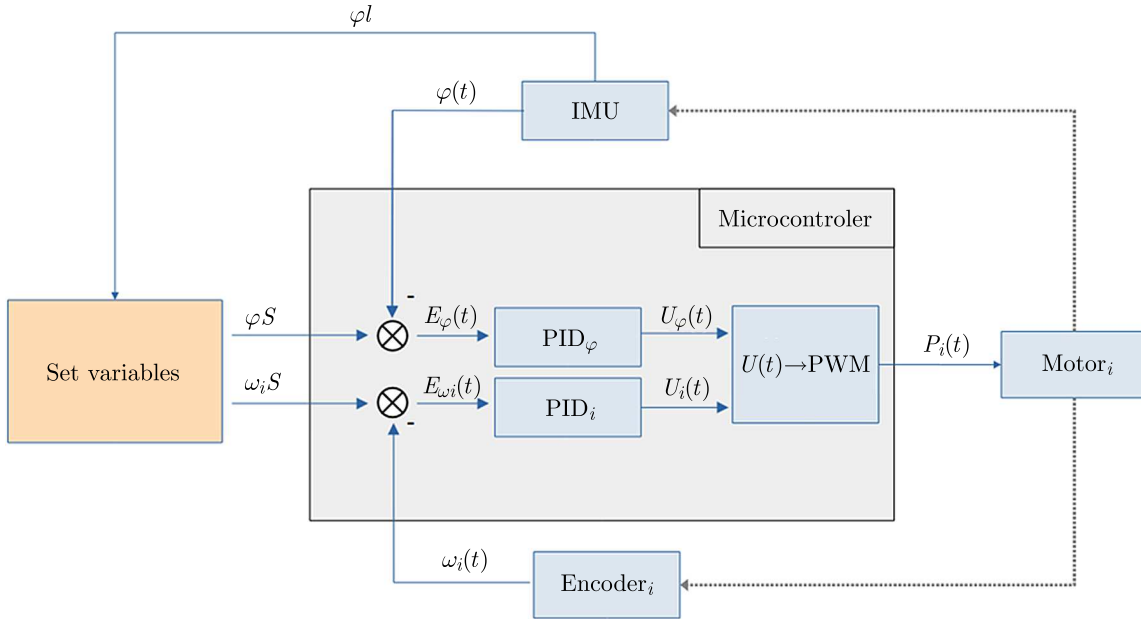


Fig. 11. Data flow diagram of the control system when using dynamic correction

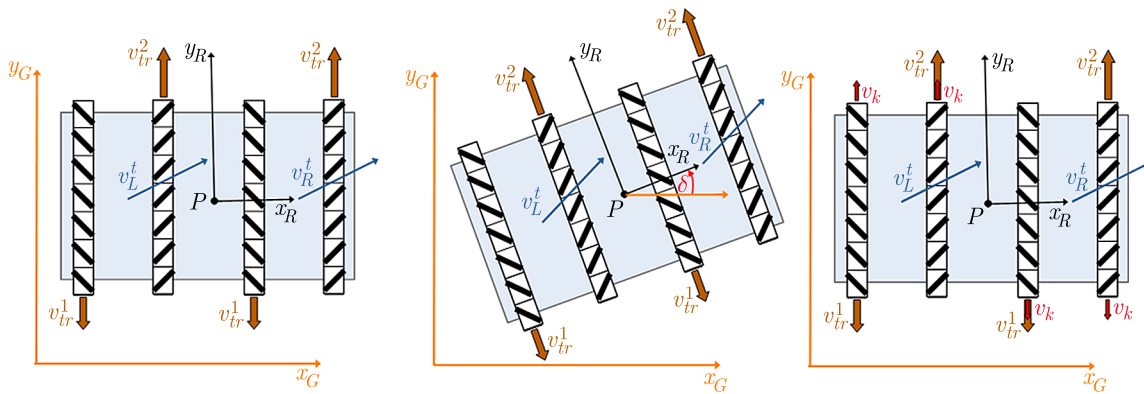


Fig. 12. Concept of dynamic correction of the movement direction. From the left: at the start of the movement, after losing the correct angular orientation of the body and after activating the correction

When moving with a fixed body orientation, the yaw angle should not change. Thanks to the data provided by the IMU sensor, information about the actual angle orientation, which determines the orientation of the vehicle on the plane, is fed into the system. Then a speed correction is introduced into the drive control system to counteract this unfavorable phenomenon. A diagram of how the correction works is presented in Fig. 12. The geometric center of omnitrack vehicles is point P . Associated with this point is a coordinate system whose y -axis coincides

with the main axis of the vehicle. When there is a change in the angular orientation of the vehicle body (due to slippage, external forces or design defects), the value of the angle δ will change, which at the beginning is 0. The angle δ is between the coordinate system at the point P and the global coordinate system, denoted by X_G, Y_G . The value of the angle δ is converted into velocity values v_k , which are added to the set linear velocities of the tracks and force orientation correction.

In order to record the trajectory of actual motion of the prototype, a measurement station was prepared, consisting of a 3000 mm \times 2400 mm measurement field, an ELP-USB4KHDR01-MFV camera mounted at a height of $h = 4070$ mm above the measurement field, and a computer for image acquisition. The stand with the prototype is shown in Fig. 13.



Fig. 13. Measurement stand of the omnidirectional vehicle

The image distortion effect seen in the camera image was removed by performing camera calibration using a charUCO card. The calibration card was a charUCO board shown in Fig. 14. It is a typical calibration checkerboard enhanced with arUCO markers. A sample arUCO marker is shown in Fig. 15. Its operation is made possible by the arUCO module, which is a part of the OpenCV open source image analysis library (<https://opencv.org/>). This module makes it convenient to work with arUCO markers, making it possible to read their position and angular orientation relative to the camera.

After the camera calibration process, a test of the measurement station was performed. Six arUCO markers with known sizes, positions and relative angular orientation were applied to an A0 sheet. Then a series of images were recorded with the calibration sheet placed in different parts of the measurement field. Exemplary images are shown in Fig. 16. Tests showed that the prepared measurement station allows recording the robot angular orientation φ_S to an accuracy of less than 1 degree and the position x_p, y_p to an accuracy of less than 0.04 m.

A single arUCO marker was placed on the body of the robot. This made it possible to read the actual position and angular orientation of the platform under test.

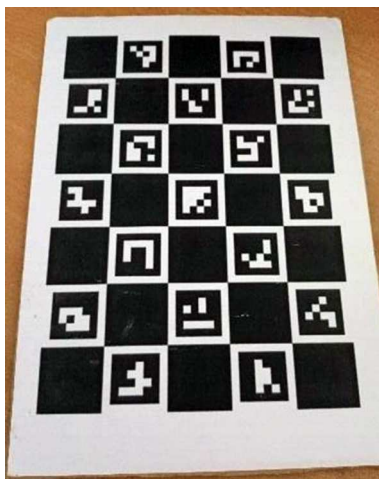


Fig. 14. CharUCO calibration card

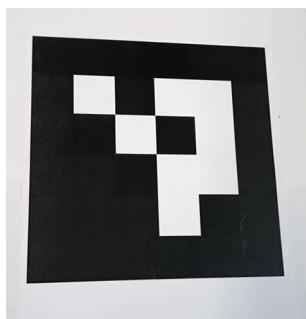


Fig. 15. arUCO marker

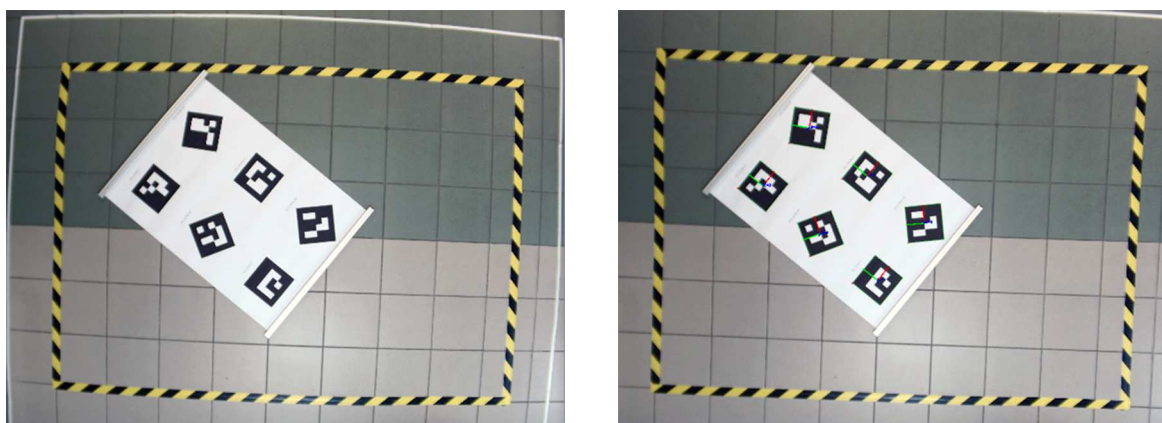


Fig. 16. Measurement field with calibration sheet before and after removal of distortion

3. Results

The prototype of the omni-tracked vehicle was used to conduct bench tests. These tests included conducting a series of test runs. During execution of the runs, the rotation of drive wheels and the angular orientation of the body were recorded by encoders and IMU sensor, and the actual position of the mobile platform was measured using the reference provided by vision system. The test runs were about 2 m in length. The measurements were compared with the results of numerical simulation. The effect of dynamic direction correction on the movement was also verified. In the type stage of the study, research of 5 ride types was conducted. Each tested drive type involved execution of 10 runs. The speed values for each drive were calculated based

on the proposed kinematic equations. The goal was to achieve movements at angles of 0, 18.44, 45, 71.56 and 90 degrees to the main axis of the platform. The theoretically calculated speed of platform movement, as well as the orientation angle of the velocity vector were compared with empirically measured values.

Table 4 collects the results of runs without correction as well as with the active drive correction system. The difference in angular deviation for runs with and without correction is shown. Standard deviations and variance were calculated for the results.

Table 4. Average angular orientation errors with respect to distance traveled for measurements that were made with and without the dynamic direction correction system. For each expected angle 10 passes were made. The highest and lowest scores were discarded

Trajectory angle φ [°]	Average orientation error δ [°/m]		Final orientation error variance σ^2		Standard deviation of final orientation error σ	
	no correction	with correction	no correction	with correction	no correction	with correction
18.44	2.60	0.81	0.05	0.22	0.22	0.47
45	1.30	0.65	0.29	0.19	0.54	0.43
71.56	3.02	0.04	0.67	0.25	0.82	0.50
90	3.79	-0.50	0.55	0.08	0.74	0.28

Statistical data shows repeatability of the measurements. Significant improvements in the driving performance can be seen when driving with the active correction system.

4. Summary, conclusions

The article deals with the control of an omni-tracked vehicle with parallel, fully overlapping tracks. A review of the literature shows the existing research gap in the issues of compensation for the unfavorable phenomenon: trajectory curvature during motion of a vehicle of this type. The equations of kinematics for controlling a single pair of parallel, fully overlapping tracks are presented. A solid model was prepared to simulate control of the presented vehicle. The simulation showed that the model with the assumed physical parameters behaved according to the proposed kinematic equations. Based on the simulation assumptions, a full-scale prototype of the omni-track vehicle was made. The kinematic scheme, design parameters and control system scheme were presented. An algorithm was proposed to dynamically compensate for the phenomenon trajectory curvature during motion. A number of test runs was carried out on a test stand equipped with a vision system. The obtained motion directions were compared with the expected values calculated on the basis of the equations of kinematics, and with the results of numerical simulation. Next, a series of test runs was carried out with the active direction correction system. These were compared with runs made without the active correction system.

The tests have shown that the proposed kinematics equations can be used to control the proposed solid model as well as actual prototype. When driving without the active correction system, there is a gradual drift of the vehicle angular orientation. As a result, the trajectory of motion becomes curved. This phenomenon is most easily noted when driving at an angle of 90, taking 3.8°/m. When using the dynamic direction correction algorithm, the phenomenon in question is significantly reduced. A several-fold improvement in the driving performance is apparent for all types of traffic studied. The smallest improvement (double) was noticed for the movement at an angle of 45 degrees. This is probably due to the way the drive is transmitted – the chain transmission has slack, which hinders the operation of the correction system. In the

remaining cases, at least a three-fold reduction in the angular orientation error was noticed. The future work will focus on detecting an active motion correction system during end-of-line motion. Tests are planned on various types of surfaces (grass, concrete, sand), as well as combined journeys, when the robot moves on several types of surfaces.

References

1. BAE J., KANG N., 2016, Design optimization of a mecanum wheel to reduce vertical vibrations by the consideration of equivalent stiffness, *Shock and Vibration*, **2016**
2. BRUTON J., 2023, Triangle Tank Version 2, <https://www.youtube.com/watch?v=rmvrlFp-qEU> (online access 17.10.2023)
3. CHEN P., MITSUTAKE S., ISODA T., SHI T., 2002, Omni-directional robot and adaptive control method for off-road running, *IEEE Transactions On Robotics And Automation*, **18**, 2
4. ENGSTRÖM J., RICHLOW E., WICKSTRÖM A., 2010, Modeling of robotic hand for dynamic simulation, Bachelor Thesis, School of Industrial Engineering and Management (ITM), MMKB 2010:23
5. FANG Y., ZHANG Y., LI N., SHANG Y., 2020, Research on a medium-tracked omni-vehicle, *Mechanical Sciences*, **11**, 137-152
6. FIEDEŃ M., BAŁCHANOWSKI J., 2021, A mobile robot with omnidirectional tracks – design and experimental research, *Applied Science*, **11**, 11778
7. FIEDEŃ M., BAŁCHANOWSKI J., 2022, Testing the driving parameters of an omni-tracked robot (in Polish), *Prace Naukowe Politechniki Warszawskiej, Elektronika*, 255-263
8. GRABOWIECKI J., 1919, *Vehicle Wheel*, US patent 1305535
9. <https://opencv.org/> (online access 17.10.2023)
10. ISODA T., CHEN P., MITSUTAKE S., TOYOTA T., 1999, Roller-crawler type of omni-directional mobile robot for off-road running, *Transactions of the Japan Society of Mechanical Engineers, ed. C*, **65**, 636
11. MORTENSEN ERNITS R., HOPPE N., KUZNETSOV I., URIARTE C., FREITAG M., 2017, A new omnidirectional track drive system for off-road vehicles, Proceedings of the XXII International Conference on “Material Handling, Constructions and Logistics”
12. PASINI D., 2019, Modelling of mobile vehicles for simulation and control, Master Degree Thesis, Politecnico di Torino
13. TADAKUMA K., TADAKUMA R., NAGATANI K., YOSHIDA K., PETERS S., UDENGAARD M., IAGNEMMA K., 2008, Crawler vehicle with circular cross-section unit to realize sideways motion, *2008 IEEE/RSJ International Conference on Intelligent Robots and Systems IROS*, 2422-2428
14. TADAKUMA K., TAKANE E., FUJITA M., NOMURA A., KOMATSU H., KONYO M., TADOKORO S., 2018, Planar omnidirectional crawler mobile mechanism – development of actual mechanical prototype and basic experiments, *IEEE Robotics and Automation Letters*, **3**, 1
15. TAHERI H., ZHAO C., 2020, Omnidirectional mobile robots, mechanisms and navigation approaches, *Mechanism and Machine Theory*, **153**
16. TAKANE E., TADAKUMA K., SHIMZU T., HAYASHI S., WATANABE M., KAGAMI S., NAGATANI K., KONYO M., TADAKORO S., 2019, Basic performance of planar omnidirectional crawler during direction switching using disturbance degree of ground evaluation method, *2019 IEEE/RSJ International Conference on Intelligent Robots and Systems IROS*, 2732-2739
17. YAMADA N., KOMURA H., ENDO G., NABAE H., SUZUMOR, K., 2017, Spiral mecanum wheel achieving omnidirectional locomotion in step-climbing, *Proceedings of the 2017 IEEE International Conference on Advanced Intelligent Mechatronics (AIM)*, 1285– 1290

18. ZHANG Y., HUANG T., 2015, Research on a tracked omnidirectional and cross-country vehicle, *Mechanism and Machine Theory*, **87**, 18-44
19. ZHANG Y., YANG H., FANG Y., 2018, Design and motion analysis of a novel track platform, *Journal of Physics: Conference Series*, **1074**

Manuscript received October 30, 2023; accepted for print January 8, 2024